

This is a postprint version of the following published document:

Díaz-Álvarez, A., Díaz-Álvarez, J., Santiuste, C., Miguélez, M. H. (2019). Experimental and numerical analysis of the influence of drill point angle when drilling biocomposites. *Composite Structures*, 209, 700–709.

DOI: <https://doi.org/10.1016/j.compstruct.2018.11.018>

© 2018 Elsevier Ltd.



This work is licensed under a [Creative Commons Attribution-NonCommercial-NoDerivatives 4.0 International License](https://creativecommons.org/licenses/by-nc-nd/4.0/).

EXPERIMENTAL AND NUMERICAL ANALYSIS OF THE INFLUENCE OF DRILL POINT ANGLE WHEN DRILLING BIOCOMPOSITES

A. Díaz-Álvarez^{1}, J. Díaz-Álvarez¹, C. Santiuste², M.H. Miguélez¹*

1 Department of Mechanical Engineering, University Carlos III of Madrid, Avda de la Universidad 30, 28911, Leganés, Madrid, Spain

2 Department of Continuum Mechanics and Structural Analysis, Universidad Carlos III de Madrid, Avda de la Universidad 30, 28911, Leganés, Spain

*Corresponding author: Phone +34916248873, andiaza@ing.uc3m.es

Abstract

Biocomposites are promising materials for traditional composites replacement in specific applications due to their interesting properties and sustainability. Although the composite components are manufactured near net shape, some machining operations, commonly drilling, are commonly required prior to mechanical joining of the components. Tool geometry, mainly the point angle of the drill, strongly affects the performance of the drilling process of composites in terms of machining induced damage.

The aim of this work is analyzing the influence of the point angle of the drill on the damage generated during drilling of 100% biodegradable composite, using both numerical and experimental approaches. The novelty of the work relies on the lack of studies of drilling 100% biodegradable composites. The influence of the point angle on the thrust forces and hence in the machining induced damage was demonstrated.

Keywords: Biocomposite; Drilling; Numerical modeling; Natural fibers; drill geometry.

1. INTRODUCTION

The use of composite materials based on natural fibers is increasing in multiple sectors in industry. In certain applications involving no critical structural requirements, they can replace synthetic composites. Due to the need of limiting the environmental impact of the production of synthetic materials certain industries as it is the case of automotive sector [1–3], propose the use of biodegradable materials. For instance, biocomposites reinforced with agave fibers are currently used in the automotive sector being their lightness and low cost particularly appreciated [4].

On the other hand, there are a wide variety of manufacturing processes in different sectors in industry producing organic waste. These residual product can be used in some cases, for the manufacture of biodegradable composites both as matrix or reinforcing fiber, for instance the lignin discarded in the manufacture of paper from wood [5], and others coming from the farms [6].

Although composite materials are intended to be manufactured near net shape, some machining operations are commonly needed in order to achieve final finishing and tolerance requirements [7] or for further mechanical joining to other components [8–12]. Drilling is the

most common operation prior to mechanical joining and has been deeply analyzed in the case of synthetic composites due to the impact of improvement of this operation in industry [13–16]. Different authors have been demonstrated the importance of the proper selection of drill geometry and cutting parameters in order to diminish machining induced damage [17–20]. Delamination is the most common defect induced during machining [21–24]. Different techniques have been used for delamination [25] measurement, ranging from the use of optical microscopy and the use of image processing techniques [26,27] to the use of thermographic and ultrasonic techniques [28,29].

There are few studies in the literature focused on drilling of 100% biodegradable materials; main contributions are briefly summarized in the following paragraphs.

Bajpai et al. [30] analyzed drilling of 100% biodegradable composite based on sisal fibers and polylactic acid (PLA) as a matrix. The influence of drill geometry and cutting parameters was analyzed showing a decrease of damage with the cutting speed, and on the contrary, an increase of machining induced defects with feed increments. It was demonstrated the strong influence of the drill geometry and the feed in the damage extension.

Díaz-Álvarez et al. [31] developed a fully biodegradable composite based on jute, cotton or flax as fibers and PLA as matrix. Drilling induced damage was analyzed through experiments testing two different geometries of drill (HSS twist drill of 118° point angle and HSS customized drill of 80° point angle, both with diameter 6mm). They observed that increments in cutting speed and feed led to a decrease in the damage extension (mainly fraying), concluding that both the geometry of the drill and the feed were the most influential parameters.

Concerning the geometry of the drill, the drill point angle is one of the most influential parameter on the cutting forces and the generation of damage in the case of synthetic composites [10]. Heisel et al. [32] analyzed the influence of the drill point angle during drilling of carbon fiber reinforced plastic (CFRP). They carried out tests with feed ranging between (0.05 – 0.40 mm/rev) and cutting speeds (21 – 513 m/min) using 6.7 mm cemented carbide drills with the same geometry and different point angles (155°, 175°, 185° and 185/178°). They concluded that the increase of point angle results in increasing feed forces; improved drill hole quality at the entrance (fraying and delamination) but diminished drill hole quality at the exit (mainly delamination). Feito et al. [8] analyzed the influence of the drill point angle and wear during CFRPs drilling. They tested 6 mm uncoated helicoidal carbide drills with 90°, 118° and 140° point angles at different values of feed (0.05, 0.1 and 0.15 mm/rev) and cutting speed (25, 50 and 100 m/min) . They concluded that thrust force depended on the point angle especially for worn tool, nevertheless, reduced influence of the point angle was observed with fresh drill. Lowest extension of delamination was obtained for lowest value of the drill point angle: delamination factor both at hole entry and exit increased with the drill point angle.

Concerning fully biodegradable composites, there is no study in the literature focused on the analysis of the influence of drill point angle during drilling of this family of materials. On the other hand, tool manufacturers provide a wide range of drill types for different applications. Despite of the interest of biodegradable composites there is no special purpose family of drills for this type of materials.

Numerical modeling of drilling process is a valuable tool for analysis of geometry influence prior to costly experiments execution. In this sense, finite element (FE) modelling has been successfully implemented in machining processes on synthetic fiber composites [33]. Traditionally, numerical simulations had been carried out using a two dimensional (2D) approach

avoiding the complexity of three-dimensional modeling (3D). 2D simulations [34], allow analyzing the orientation of the fibers, the cutting parameters and materials properties in different composites [35–37], however it is not possible to reproduce out-of-plane failure mechanisms [38], and cannot be applied to the modelling of complex cutting processes [39], such as the current drilling processes in industrial applications. The first works on the development of 3D models of the drilling process attempted to find the relationship of the delamination during the drilling of CFRPs with the thrust force and the influence of the point angle on the generation of the damage, using a simplified approach considering the drill as a punch [20,40,41]. The simulation of the penetration of the drill in the material and the failure mechanism implies the use of 3D models that enable the simulation of the chip removal [42–44].

The simulations related to fully biodegradable materials have focused on determining main mechanical properties, with few works focused on modelling of the machining processes [45,46]. It should be noted that up date, just a previous work of the authors dealing with numerical modelling of drilling operation on 100% biodegradable composites is available.

This paper focuses on the analysis and study of the influence of drill point angle in drilling performance of 100% biodegradable composite. 3D FE model has been developed and validated in a previous work for the simulation of the drilling process on fully biodegradable material (Flax as fibers and PLA as matrix) in different conditions. The model has been used to determine the value of the drill point angle (in the range 70-118°) giving best results in terms of thrust force and machining damage. Uncoated HSS twist drills were manufactured in order to validate the results obtained numerically. The model showed good accuracy in simulation of drilling and the influence of the drill point angle on the thrust force and damage generation was demonstrated.

2. NUMERICAL MODELING

2.1. DRILLING MODEL

The numerical model has been developed and validated in a previous work focused on the simulation of the drilling process of fully biodegradable material (Flax as fibers and PLA). Two different drill geometries (HSS twist drill and HSS customized drill) were tested on variable composite thickness.

The 3D model is able to reproduce the complete movement of the drill, including the spindle speed, the feed rate and the chip removal simulating the penetration of the tool in the material. The extension of the workpiece modelled is a cylinder of diameter 10 mm, corresponding to the free surface inside the supporting back plate used in experimental tests. During the experimental tests, it was demonstrated that drilling induced damage was inside the free surface of diameter 10 mm around the hole.

Different point angles of 118°, 110°, 100°, 90°, 80° and 70° for a standard HSS twist drill of 6 mm diameter has been simulated, the selected geometry was as simple as possible, in order to obtain a better understanding of the effect of the point angle. The selected values are in the range of those provided by the tool manufacturer. The values higher than 118° are only recommended for very hard cutting, while point angle lower than 70° are related to excessive weakness of the tools. The material has been simulated in different thicknesses of the composite BF/PLA10 (Flax fibers and PLA 10361D matrix) were simulated (2 layers, 1.4 mm; 3 layers, 2.14

mm; and 4 layers, 2.68 mm). *Figure 1* illustrates the scheme of the drilling model, as well as the different drill point angles analyzed.

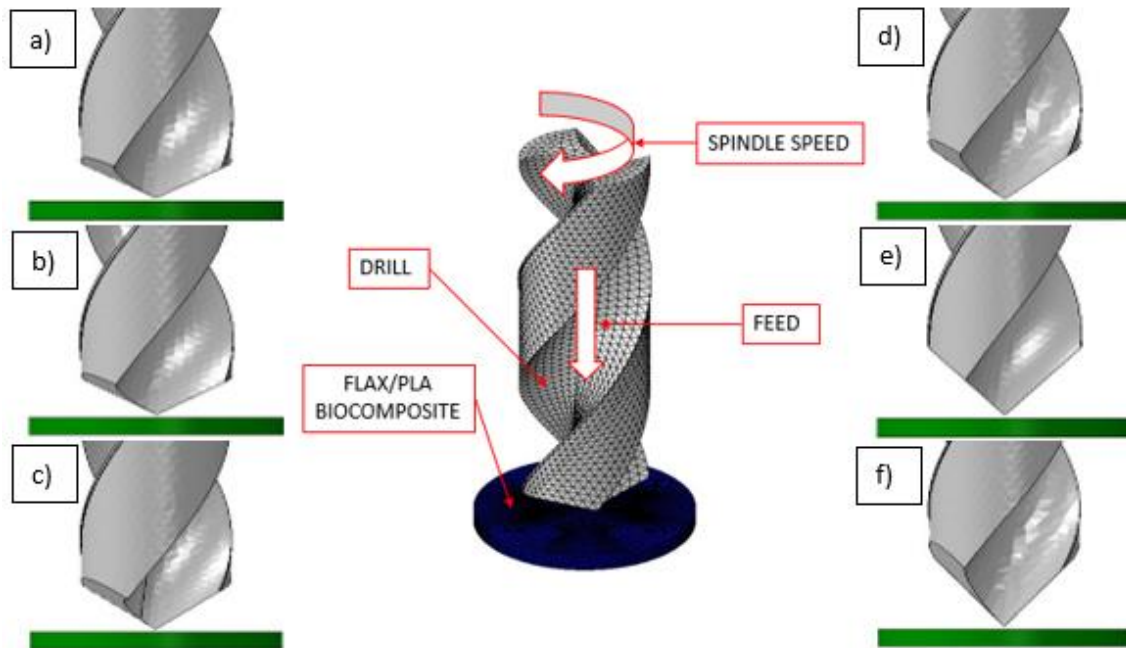


Figure 1. Scheme of the drilling model. Different drill point angles: a) 118°, b) 110°, c) 100°, d) 90°, e) 80° and f) 70°.

An interaction contact has been defined between the drill and the the workpiece. The contact between the surface of the drill and the node region corresponding to the composite has been formulated through a kinematic contact, available in ABAQUS/Explicit [47].

The selection of the element size for both the drill and the material require a compromise between the computational cost and the accuracy of the simulation. Hexagonal CRD8R element type (prismatic elements with hexagonal section) with size 120 μm was chosen for the composite modeling, diminishing the dependence of the results with the mesh orientation in the laminate plane. In the case of drill, it has been imported to ABAQUS from the CAD program, and was modeled to behave rigid, using a rough mesh, based on triangular elements type R3D3 with size 500 μm .

2.2. MATERIAL MODELING

The mechanical response of the workpiece material was modeled through a rheological model calibrated and validated in a previous work [46]. This constitutive model accounts for the plastic behavior, as well as the effect of the strain rate on the fully biodegradable composite material. It was calibrated through the comparison with experimental stress-strain curves and relaxation tests performed on the material, taking into account the influence of the strain rate.

Figure 2 shows the effect of the strain rate through different stress-strain curves, according to which, when the strain rate increases, both the resistance and the stiffness are enhanced while the ultimate strain is decreased.

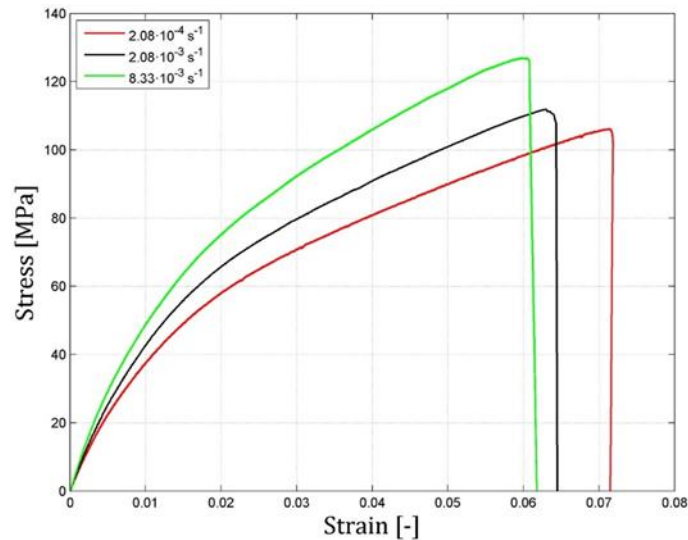


Figure 2. Stress-strain curves obtained experimentally under different strain rates [46].

Both the yield stress and the plastic behavior of the biodegradable compound were determined as a function of the strain rate following the corresponding stress-strain curve. It was necessary to perform an interpolation for different values of strain rate.

In order to simulate chip removal, a VUSDFLD subroutine has been implemented, allowing the erosion of the elements once the ultimate strain is reached, defined as a function of the strain rate. Thus, for the chip removal during the simulation, the subroutine firstly evaluates the strain rate, and continues with the calculation of the ultimate strain. When the strain level in one of the three main directions is higher than the value of the ultimate strain previously calculated the element is eroded.

Main damage mechanism during drilling of 100% biodegradable materials is fraying, while delamination has not been observed during previous experimental tests on this type of material [31], thus the cohesive elements for debonding between plies simulation are not required in this model.

3. EXPERIMENTAL WORK

3.1. MANUFACTURING

Fully biodegradable composite material has been manufactured based on flax fibers and PLA 10361D matrix through the compression molding method. Flax fibers are one of the earliest natural fibers [48] and they are currently used in the composite industry [49–51]. Basket weave flax (BF) used as reinforcement for the manufacture of the 100% biodegradable composites have been cut into plates of 150 x 150 mm with an areal density of 463.3 g/m², 0.94 mm thickness and no chemical pre-treatment. On the other hand, a thermoplastic resin PLA 10361D provided by Nature Works, LLC, in pellets shape, has been used as a matrix. The polymer of PLA 10361D has a density of 1.24 g/cm³ and a melting temperature around 145-170 °C, which is created specifically for use as a binder for natural fiber composite manufacture.

The manufacture route of the composite material by the method of compression molding involves different stages of pressure and heat. Firstly, the PLA is kept in an oven at 95° for 30 minutes to remove the possible water content, to subsequently, obtain PLA films from the

pellets, keeping them at 185° for 3 minutes between thermo-heated plates. Once cooled, and with a dimension of 160 x 200 mm², the PLA films are alternately stacked with the woven plies and placed between the thermo-heated plates at 185° for 2 minutes. After preheating, a pressure of 16 MPa is applied for 3 minutes by means of a universal testing machine, and later, they are dried at room temperature. *Figure 3* illustrates the outline of the biocomposite manufacture through compression molding method.

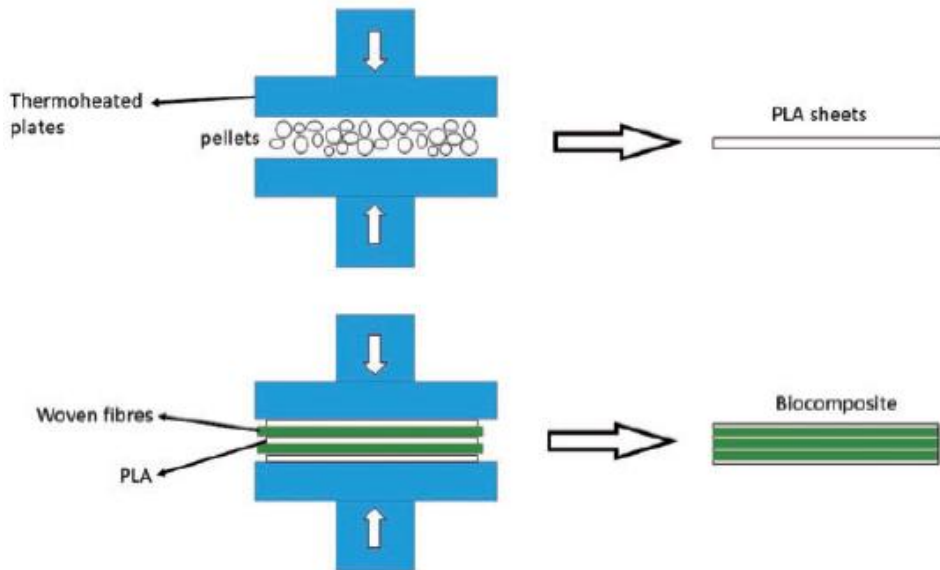


Figure 3. Flax/PLA (BF/PLA10) biocomposite manufacture route through compression molding method [31].

Biocomposite samples for the drilling tests have been manufactured with different thicknesses (two, three and four layers) and subsequently cut in rectangular specimens 120 x 30 mm² allowing the attachment inside the confining device.

According to ATM D2584 standard, the weight ratio was controlled by different thickness of PLA films, being 58.6% the resulting fiber volume fraction for flax/PLA composites. The tensile strength for the manufactured biocomposite have been obtained testing the specimens in an Instron 8516 universal testing machine, according to the ATM D3039 standard (*Table 1*). More details for the manufacture of biodegradable composites and their mechanical properties can be found in [52].

Table 1. Tensile strength for the Flax/PLA composite [52].

<i>Material</i>	<i>Tensile strength (MPa)</i>	<i>Standard deviation (MPa)</i>	<i>Elastic modulus (GPa)</i>	<i>Ultimate strain</i>
<i>Flax/PLA</i>	104.0	4.71	7.84	0.069

3.2. DRILLING TESTS

Drilling tests were carried out in a B500 KONDISA machining center, instrumented with a rotary dynamometer (Kistler 9123C) for the measurement of thrust forces and torque (see *Fig. 4*). A confinement device has been installed in order to clamp the sample to be drilled (which has the dimensions of 120 mm x 30 mm). Moreover the chips are evacuated generating a suction current with a vacuum connected to the confining device avoiding the dispersion of the fibers. The drilling device consists of a 100 x 80 x 52 mm³ aluminum main body, with two plates inside,

sliding the upper one over rectified guides to ensure the accuracy of the drill and allowing the samples to be attached during drilling (*Figure 1 and 4.a*). In addition, the back plate presents a hole of 10 mm providing free surface for drilling the hole.

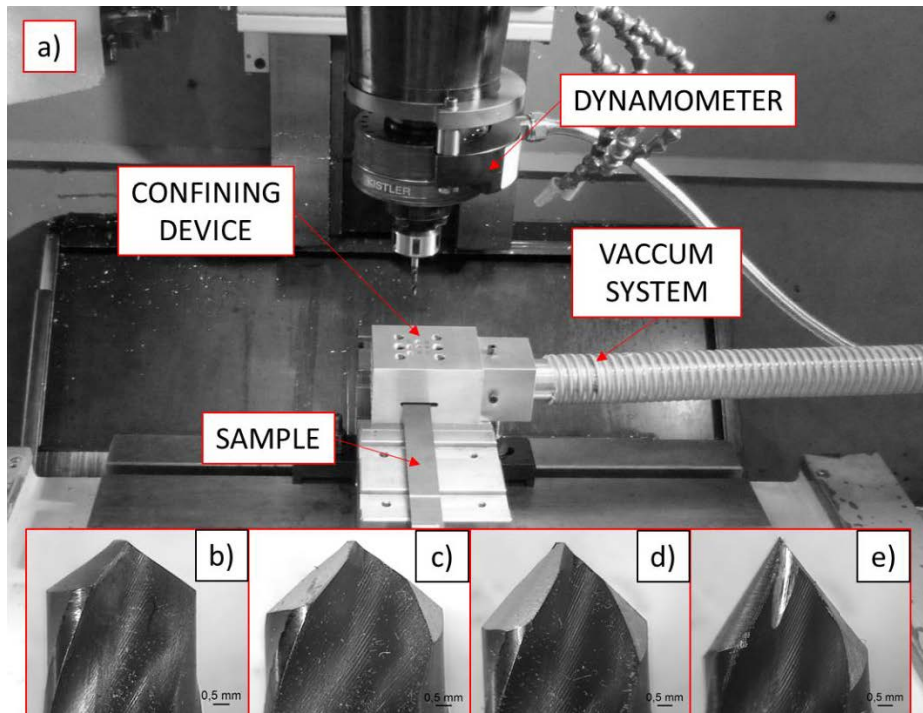


Figure 4. a) Configuration used in the machining center B500 Kondia during drilling tests; b) 118°; c) 100°; e) 90° and e) 70°

Cutting parameters used during the experimental tests have been selected taking into account the tool manufacturer recommendations for the biodegradable composites and the literature [30]. The experimental tests have been carried out at three cutting speeds (15, 20 and 25 m/min) and three feeds (0.03, 0.06 and 0.12 mm/rev) in dry conditions. To perform the tests, HSS twist drills with point angles of 118°, 100°, 90° and 70° were manufactured in order to validate the results obtained numerically, one fresh drill was used in each test to guaranty the integrity of the cutting edges.

Damage extension was quantified in terms of the damage factor (F_d) defined as the ratio between the maximum diameter of damaged zone, and the nominal diameter of the hole (drill diameter), see *Figure 5*. Damage factor was quantified both at the entrance (peel up) and the exit (push out) of the drill through the images obtained with the optical microscope Optika SZR. Further details of the damage analysis derived from drilling process on the flax biocomposite material can be found in [31].

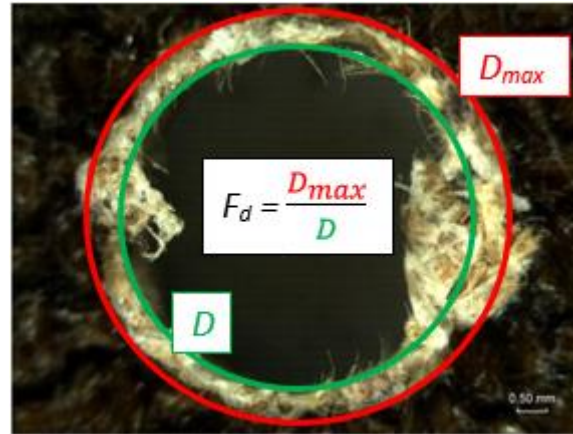


Figure 5. Image taken with Optika SZR microscope for the Damage factor (F_d) calculation for flax biocomposite (three layers) drilled at 20 m/min and 0.06 mm/rev (push out).

4. NUMERICAL RESULTS

Simulation of drilling was carried out for the tip angles of 118°, 110°, 100°, 90°, 80° and 70°. Different values of the number of layers and cutting parameters were modeled being summarized in the Table 2.

Table 2. Different cases analyzed numerically for each point angle (118°, 110°, 100°, 90°, 80° and 70°) study during the drilling of flax biocomposite.

Case	Layers	V [m/min]	f [mm/rev]
Case 1	2	20	0.03
Case 2			0.06
Case 3			0.12
Case 4	3	15	0.06
Case 5		25	
Case 6	4	20	0.06
Case 7	3		

The influence of point angle during drilling was analyzed in terms of the induced damage (peel up and push out) and thrust forces generated during the process.

Figure 6 shows the numerical thrust forces predicted for the different cases proposed.

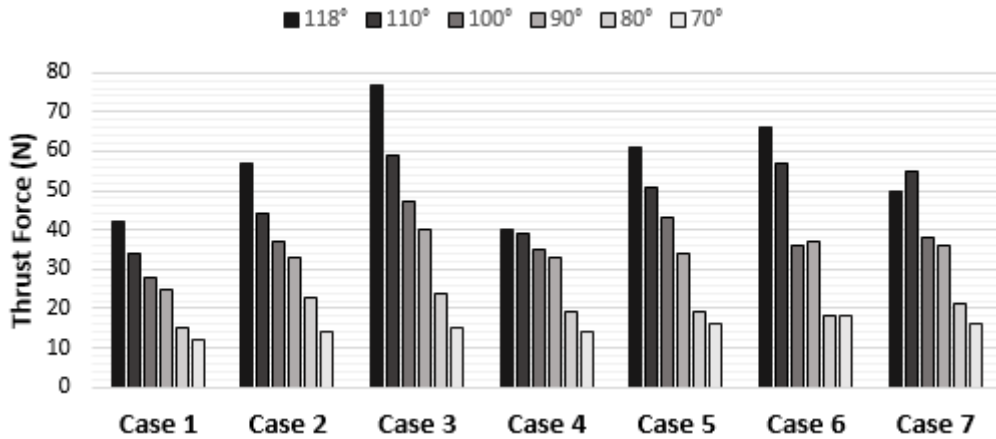


Figure 6. Maximum numerical Thrust Forces results for the different drill point angles analyzed: 118°, 110°, 100°, 90°, 80° and 70° (HSS twist drill of 6 mm diameter).

The increase of the drill point angle leads to the increment of the thrust forces in all cases analyzed. This trend is in agreement with the observations of other authors during drilling of other types of composite materials (see for instance [8,32]). In addition, the effect of the drill point angle was more significant when the feed was incremented. Comparing the Case 1 with the Case 3 (at the same cutting speed), it can be appreciated an increment of the thrust force when the drill point angle change from 70° to 118° up to 250 % and 400 % respectively for Cases 1 and 3.

The effect of drill point angle combined with the variation of cutting speed on the thrust force was no as relevant as the effect of the feed, however, the larger the cutting speed used the larger the thrust force found.

Independently of the drill point angle, and for the studied conditions, the numerical model shows a negligible effect of the number of layers on the thrust forces.

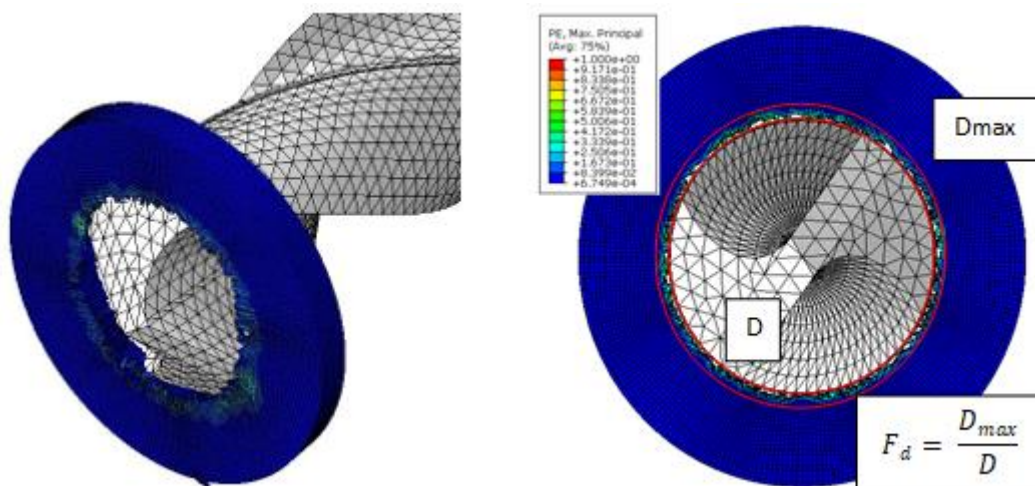


Figure 7. Scheme of Numerical quantification of the damage factor (F_d) (HSS twist drill of 118° point angle for Case 3).

Damage factor was obtained using the post processing module ABAQUS CAE (Figure 7) by means of the extension of plastic deformation generated in the flax composite during the simulation

both at the entry (peel up) and at the exit (push out). In *Figure 8*, the damage generated during the drilling of the flax biocomposite at the entry (peel up) is shown.

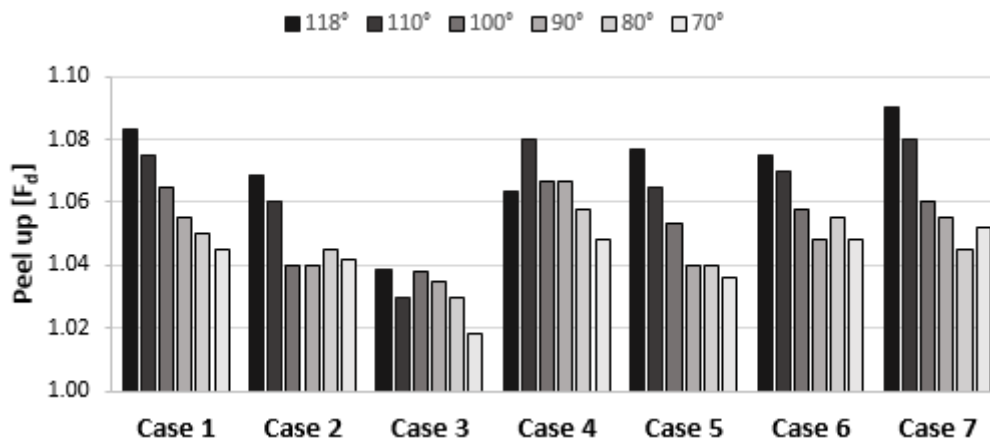


Figure 8. Damage factor (F_d) obtained numerically for both drill point angles (118° , 110° , 100° , 90° , 80° and 70°) at the entry (peel up).

For all tested conditions, the decrease of the drill point angle led to decreased damage extension at the entry (peel up) during drilling. Therefore, the best results are those obtained for the drill point angles of 90° , 80° and 70° in all cases analyzed.

Concerning the values obtained for the damage generated at the exit (push out) of the drill, (*Figure 9*) the same trend is observed: the best values are obtained with the lowest drill point angle (90° , 80° and 70°), improving those obtained with respect to the worst (118° and 110°) up to 3.5 % in the Case 4.

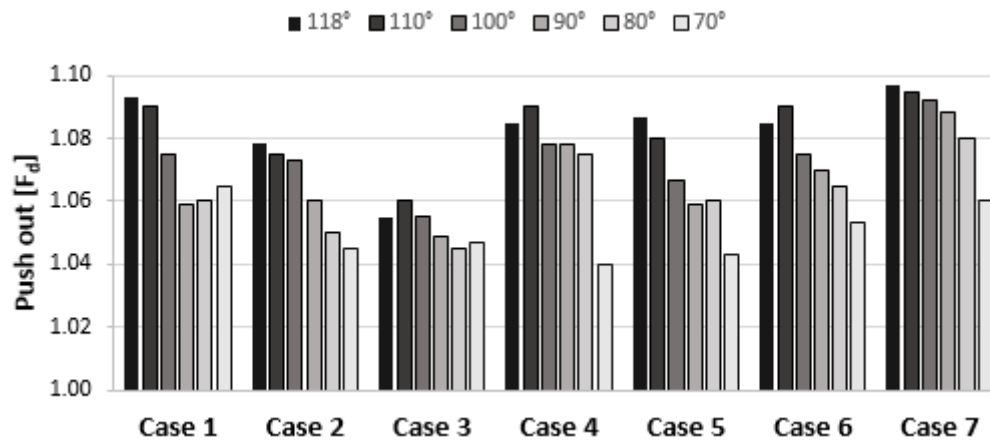


Figure 9. Damage factor (F_d) obtained numerically for both drill point angles (118° , 110° , 100° , 90° , 80° and 70°) at the exit (push out).

The damage extension is greater at the hole exit in all cases for the same testing conditions (*Figure 8 and 9*). This behavior is also observed in synthetic composites where the critical damage extension commonly appears at the hole exit.

Concerning the influence of cutting parameters, it is observed from cases Case 1, 2 and 3 (with cutting speed fixed at 20 m/min and the feed changing from 0.03 to 0.12 mm/rev) that the increment in the feed results in a decrease of the damage generated during the drilling (*Figure*

10. a) and b)). This trend is contrary to the results obtained during drilling of synthetic composite [17,53–55], however this behavior is consistent with the viscoelastoplastic behavior of these materials reported in [31]. In addition, it is observed that the point angle effect is more significant for small feeds in the Case 1 going from 70° to 118°, where the damage at the entrance and exit increased 3.6 % and 2.6 % respectively. However, in the Case 3, with cutting speed equal to that in the Case 1 but with increased feed, increments of 1.93 % and 0.76 % were obtained for the peel up and push out respectively, when increasing the angle from 70° to 118°. Thus, no clear trends can be identified in the effect of the point angle with the cutting speed on the damage generated both at the peel up and push out.

Independently of the drill point angle, the numerical model showed negligible effect of the number of layers on the damage at the entry and exit zone.

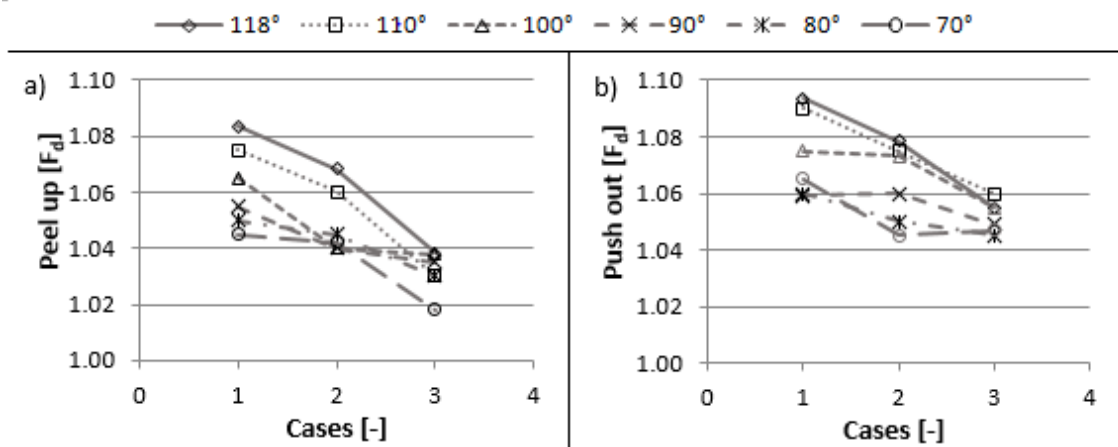


Figure 10. Damage factor (F_d) at entry (a)) and exit (b)) of the drill for each drill point angle (118°, 110°, 100°, 90°, 80° and 70°) for Cases 1, 2 and 3 (cutting speed fixed at 20 m/min and feeds of 0.03, 0.06 and 0.012 mm/rev.

5. EXPERIMENTAL RESULTS

The numerical analysis showed the influence of the point angle, being 70° the best option in terms of the thrust force and drilling induced damage. In this section, further experimental analysis is presented with the aim of validating numerical results. A selection of cases analyzed in the numerical study were reproduced (see Table 2). With this objective, HSS twist drills (6 mm diameter) with different point angles (118°, 100°, 90° and 70°) corresponding to the extreme and medium values of the range analyzed numerically were manufactured.

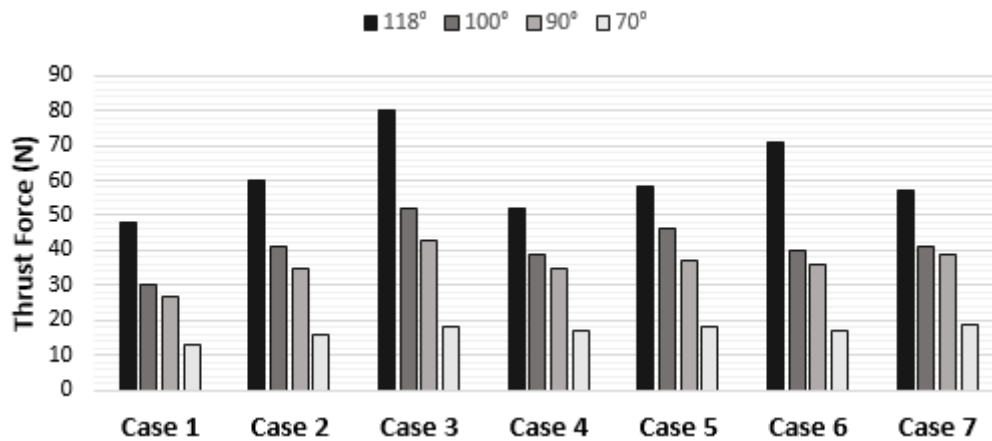


Figure 11. Maximum experimental Thrust forces for the different point angles studied (118°, 110°, 100°, 90°, 80° and 70°).

Figure 11 illustrate the maximum values of thrust forces obtained during experiments: in agreement with the numerical results, it is observed that the larger point angle resulted in greater thrust force (obtaining the lowest values for a point angle of 70°). Thus, for the point angle of 70° the value of the thrust force was diminished up to 77.5% when compared with the force obtained for the tip angle 118° (Case 3, 20 m/min and 0.06 mm/rev). These results agree with those obtained by other authors during the experimental analysis of the influence of the drill point angle [8,32].

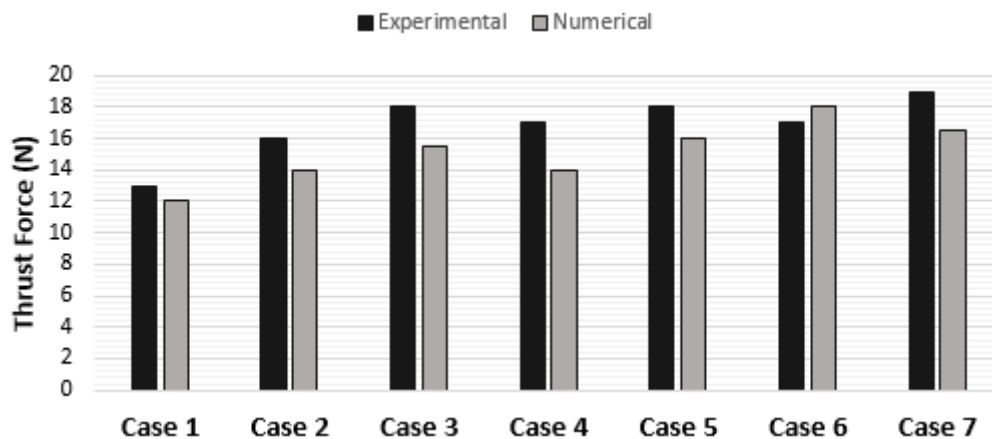


Figure 12. Comparison of numerical and experimental Thrust Force results for 70° drill point angle.

Reasonably accuracy in the prediction of the thrust force was observed (Figure 12). Therefore, the best result has been obtained for Case 6 (20 m/min, 0.06 mm/rev and 3 layers), in which the error presented the lowest value (about 5%). The largest value of the error (about 13 %) was obtained for the Case 3 (20 m/min, 0.06 mm/rev and 2 layers). These values of error are in the order of those reported in the literature during numerical modeling of cutting [39].

Figure 13 summarizes the experimental results of the damage factor measured at the entrance of the drill (peel up) for the different cases studied.

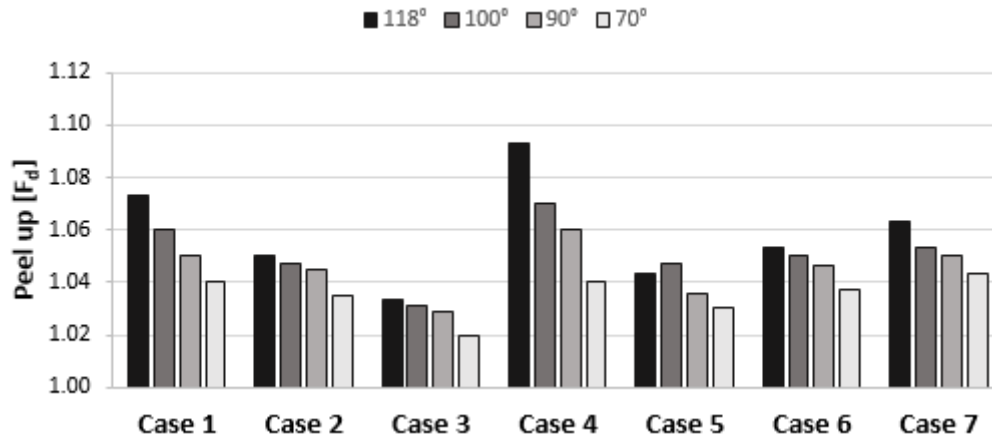


Figure 13. Experimental Damage factor at the entrance of the drill (peel up) for the different cases analyzed experimentally.

In agreement with numerical results the smallest value of damage factor at the entry (peel up) was obtained for the lower value of the drill point angle (70°) in all cases analyzed. Moreover, it can be seen that the best results were obtained at high cutting speed and feed for two layers (Case 3), and the worst, were obtained at low cutting speed and two layers.

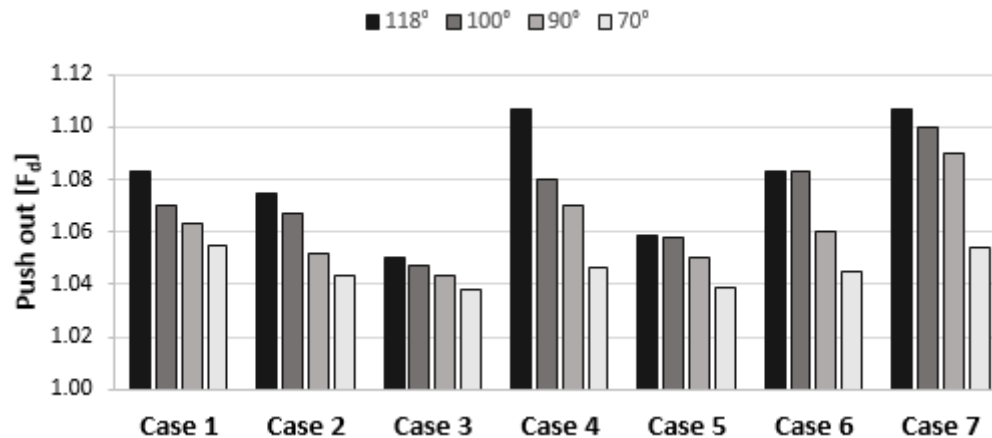


Figure 14. Experimental Damage factor at the entrance of the drill (push out) for the different cases analyzed experimentally.

The damage factor at the hole exit (push out) is presented in the Figure 14. Similar trend to that observed at the hole entry was found. This tendency (both peel up and at push out) is contrary to the results obtained during drilling of synthetic composite [8,32], but on the other hand, consistent with the results found in previous work focused on biocomposites due to the viscoelastoplastic behavior of these materials [31].

Concerning the influence of the feed on the damage, the increment of the feed (from 0.03 to 0.12 mm/rev, and fixed cutting speed equal to 20 m/min, corresponding with Cases 1, 2, 3) resulted in a decrease in the damage generated for all the cases studied (118°, 100°, 90° and 70°). and varying the feed, These results corroborate those obtained from the literature when drilling fully biodegradable materials [31]. This trend is also illustrated in Figure 15.

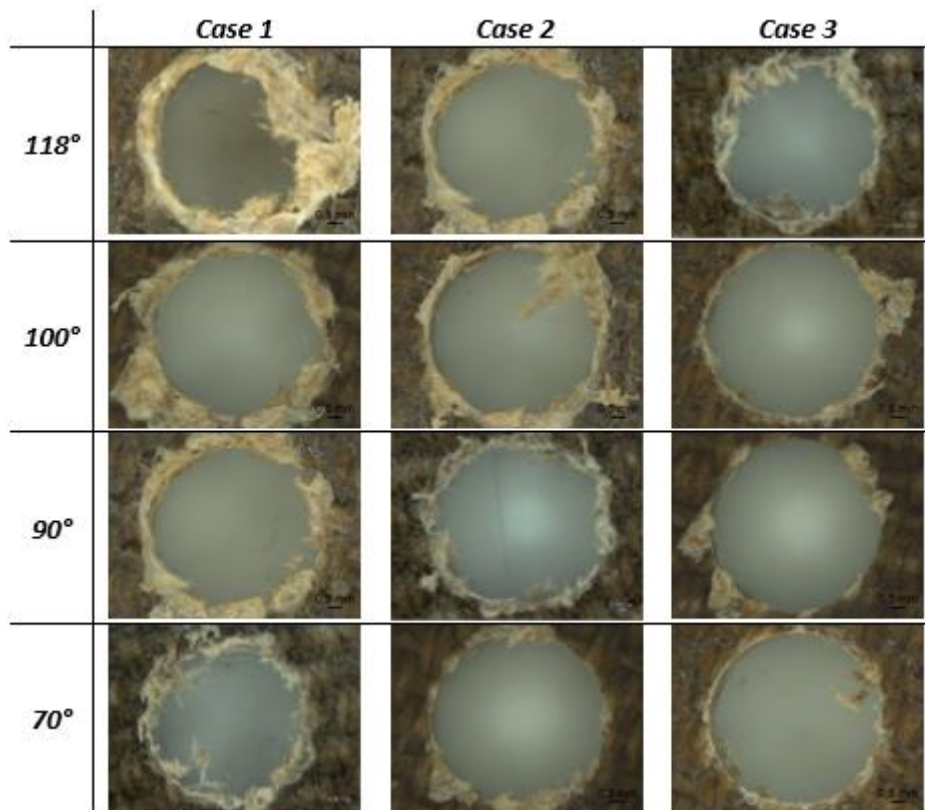


Figure 15. Microscope images (Optika SZR) for different drill point angles (118°, 110°, 100°, 90°, 80° and 70°) at the exit (push out); Cases 1, 2 and 3 (20 m/min cutting speed and feeds of 0.03, 0.06 and 0.12 mm / rev respectively).

Figure 16 shows the comparison for the damage results from the drilling process, both at the entry (peel up) and at the exit (push out) for a drill point angle of 70° the most favorable geometry for hole quality. .

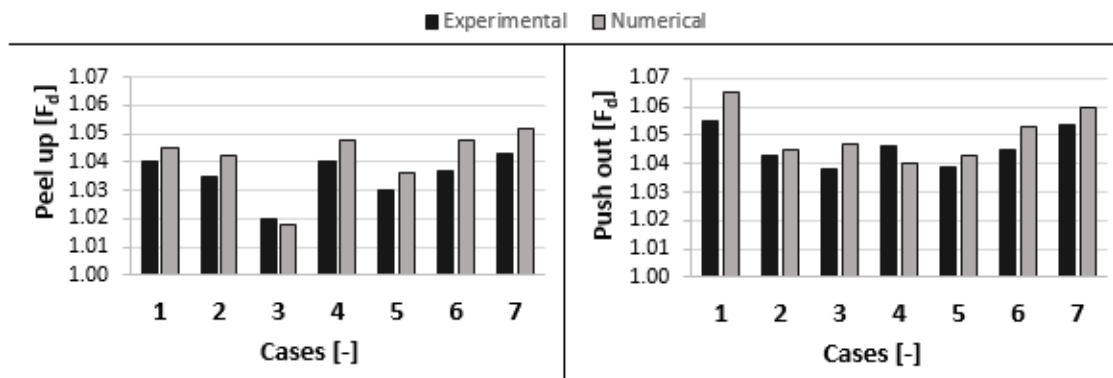


Figure 16. Comparison of Damage Factor (F_d) results obtained numerically and experimentally for 70° drill point angle.

The drilling model accurately predicts the damage factor, obtaining higher push out damage than peel up in all the cases studied for a 70° drill point angle. For the entry damage factor, the maximum error was about 1.1%, obtained for the Case 6 while, the minimum value was obtained for Case 3, with an error about 0.2%. Regarding the push out damage, the error obtained follows the same trend, showing the highest value for Case 1 with 1% and the lowest error value about 0.2% for the Case 2.

6. CONCLUSIONS

This paper has been focused on the influence of the drill point angle during drilling of flax/PLA biocomposites. Main contributions of the analysis are summarized below:

- A 3D numerical model of the drilling process on flax-based composite developed and validated in a previous work, has been used to analyze the effect of the drill point angle (118°, 110°, 100°, 90°, 80° and 70°) during the drilling process. The 3D model allows the simulation of drill movement and chip removal.

- The numerical model allows the accurate prediction of the damage factor for each value of drill point angle, demonstrating the clear influence of drill point angle. The increase of the angle resulted in increased damage extension.

- The numerical results follow the trend observed in previous experimental work of the authors, according to which, increments in the feed led to damage reduction, contrary to the tendency obtained in drilling of synthetic composites.

- A greater influence of the point angle of the tool was observed in the feed forces recorded with small feed values (3.6 % peel up and 2.6 % push out). On the other hand, the effect of the drill point angle on the damage both at the entry and exit was reduced for higher feeds (1.93 % and 0.76 % respectively).

- HSS twist drills with point angles of 118°, 100°, 90° and 70° have been manufactured in order to validate the result obtained numerically. The experimental tests corroborate the numerical damage predictions, showing good accuracy of the numerical model with error values ranging between 0.2 and 1.1% in all the cases in the range analyzed.

- Both the model and the experiments showed higher point angles inducing higher values of thrust force and on the contrary, a reduction of the damage generated during the machining process. This decrease in the generated damage, is contrary to the results obtained by other authors for synthetic composite, due to the viscoelastoplastic behavior of the biodegradable composites.

Despite the promising results obtained in the work, the limitations of the study should be accounted. Firstly, the analysis was carried out in a certain range of tip angle and cutting parameters similar to those recommended for other synthetic composites. The lack of studies focused on drilling of biocomposites did not allow the extensive revision of proper references. On the other hand, the study has been focused on the analysis of fresh drill performance, meaning that the evolution of tool wear has not been accounted. The optimization of drill geometry should take into account also the evolution of wear. Acute drill geometries are related to enhanced drill weakness and high rates of wear, thus these results concerning drilling performance should be completed with the analysis of wear progression.

ACKNOWLEDGMENTS

The authors acknowledge the financial support to the Ministry of Economy and Competitiveness of Spain and FEDER program through the projects DPI2017-89197-C2-1-R and DPI2017-89197-C2-2-R.

REFERENCES

- [1] Ahmad F, Choi HS, Park MK. A review: Natural fiber composites selection in view of mechanical, light weight, and economic properties. *Macromol Mater Eng* 2015;300:10–24. doi:10.1002/mame.201400089.
- [2] Li Y, Mai YW, Ye L. Sisal fibre and its composites: a review of recent developments. *Compos Sci Technol* 2000;60:2037–55. doi:10.1016/S0266-3538(00)00101-9.
- [3] Omrani E, Menezes PL, Rohatgi PK. State of the art on tribological behavior of polymer matrix composites reinforced with natural fibers in the green materials world. *Eng Sci Technol an Int J* 2016;19:717–36. doi:10.1016/j.jestch.2015.10.007.
- [4] Mancino A, Marannano G, Zuccarello B, Mancino A. Implementation of eco-sustainable biocomposite materials reinforced by optimized agave fibers *Procedia Struct. Integrity* 2018;0. doi:10.1016/j.prostr.2017.12.052.
- [5] Yamini G, Shakeri A, Zohuriaan-mehr MJ, Kabiri K. Cyclocarbonated lignosulfonate as a bio-resourced reactive reinforcing agent for epoxy biocomposite : From natural waste to value-added bio- additive. *J CO2 Util* 2018;24:50–8. doi:10.1016/j.jcou.2017.12.007.
- [6] Yzombard A, Gordon SG, Miao M. Morphology and tensile properties of bast fibers extracted from cotton stalks. *Text Res J* 2013;84:303–11. doi:10.1177/0040517513495949.
- [7] Voss R, Seeholzer L, Kuster F, Wegener K. Influence of fibre orientation, tool geometry and process parameters on surface quality in milling of CFRP. *CIRP J Manuf Sci Technol* 2017;18:75–91. doi:10.1016/j.cirpj.2016.10.002.
- [8] Feito N, Díaz-Álvarez J, Díaz-Álvarez A, Cantero JL, Miguélez MH. Experimental analysis of the influence of drill point angle and wear on the drilling of woven CFRPs. *Materials (Basel)* 2014;7:4258–71. doi:10.3390/ma7064258.
- [9] Feito N, Díaz-Álvarez J, Cantero JL, Miguélez MH. Influence of Special Tool Geometry in Drilling Woven CFRPs *Materials*. *Procedia Eng* 2015;132:632–8. doi:10.1016/J.PROENG.2015.12.541.
- [10] Grilo TJ, Paulo RMF, Silva CRM, Davim JP. Experimental delamination analyses of CFRPs using different drill geometries. *Compos Part B Eng* 2013;45:1344–50. doi:10.1016/j.compositesb.2012.07.057.
- [11] Kang J, Rao H, Zhang R, Avery K, Su X. Tensile and fatigue behaviour of self-piercing rivets of CFRP to aluminium for automotive application. *IOP Conf Ser Mater Sci Eng* 2016;137. doi:10.1088/1757-899X/137/1/012025.
- [12] Wahab MA. *Joining Composites With Adhesives* 2016.
- [13] Rodríguez-Barrero S, Fernández-Larrinoa J, Azkona I, López De Lacalle LN, Polvorosa R. Enhanced Performance of Nanostructured Coatings for Drilling by Droplet Elimination. *Mater Manuf Process* 2016;31:593–602. doi:10.1080/10426914.2014.973582.
- [14] López De Lacalle LN, Rivero A, Lamikiz A. Mechanistic model for drills with double point-angle edges. *Int J Adv Manuf Technol* 2009;40:447–57. doi:10.1007/s00170-007-1362-8.
- [15] Xu J, Li C, Mi S, An Q, Chen M. Study of drilling-induced defects for CFRP composites using new criteria. *Compos Struct* 2018;201:1076–87. doi:10.1016/j.compstruct.2018.06.051.

- [16] Kumar K, Palaniyandi K. Drilling on fiber reinforced polymer / nanopolymer composite laminates : a review. *Integr Med Res* 2017;7:180–9. doi:10.1016/j.jmrt.2017.06.003.
- [17] Díaz-Álvarez A, Rodríguez-Millán M, Díaz-Álvarez J, Miguélez MH. Experimental analysis of drilling induced damage in aramid composites. *Compos Struct* 2018;1–9. doi:10.1016/j.compstruct.2018.05.068.
- [18] Davim JP, Rubio JC, Abrao AM. A novel approach based on digital image analysis to evaluate the delamination factor after drilling composite laminates. *Compos Sci Technol* 2007;67:1939–45. doi:10.1016/j.compscitech.2006.10.009.
- [19] Tsao CC, Hocheng H. Effect of tool wear on delamination in drilling composite materials. *Int J Mech Sci* 2007;49:983–8. doi:10.1016/j.ijmecsci.2007.01.001.
- [20] Luís Miguel P. Durão, Daniel J.S. Gonçalves, João Manuel R.S. Tavares, Victor Hugo C. de Albuquerque, A. Aguiar Vieira, A. Torres Marques. Drilling tool geometry evaluation for reinforced composite laminates. *Compos Struct* 2010;92:1545–50. doi:10.1016/j.compstruct.2009.10.035.
- [21] Qiu X, Li P, Li C, Niu Q, Chen A, Ouyang P, et al. Study on chisel edge drilling behavior and step drill structure on delamination in drilling CFRP. *Compos Struct* 2018;203:404–13. doi:10.1016/j.compstruct.2018.07.007.
- [22] Hocheng H, Chen CC, Tsao CC. Prediction of critical thrust force for tubular composite in drilling-induced delamination by numerical and experimental analysis. *Compos Struct* 2018;203:566–73. doi:10.1016/j.compstruct.2018.07.051.
- [23] Jahanian E, Zeinedini A. Influence of drilling on mode II delamination of E-glass / epoxy laminated composites. *Theor Appl Fract Mech* 2018;96:398–407. doi:10.1016/j.tafmec.2018.06.002.
- [24] Joshi S, Rawat K, Balan ASS. A novel approach to predict the delamination factor for dry and cryogenic drilling of CFRP. *J Mater Process Tech* 2018;262:521–31. doi:10.1016/j.jmatprotec.2018.07.026.
- [25] Davim JP, Reis P. Study of delamination in drilling carbon fiber reinforced plastics (CFRP) using design experiments *Compos Struct* 2003;59:481–7.
- [26] Khashaba UA. Delamination in drilling GFR-thermoset composites. *Compos Struct* 2004;63:313–27. doi:10.1016/S0263-8223(03)00180-6.
- [27] Krishnamoorthy A, Mercy JL, Vineeth KSM, Kumar M. Delamination Analysis of Carbon Fiber Reinforced Plastic (CFRP) Composite plates by Thermo graphic technique. *Mater Today Proc* 2015;2:3132–9. doi:10.1016/j.matpr.2015.07.101.
- [28] Tsao CC, Hocheng H. Computerized tomography and C-Scan for measuring delamination in the drilling of composite materials using various drills. *Int Jmach Tool Manu* 2005;45:1282–7. doi:10.1016/j.ijmachtools.2005.01.009.
- [29] Faria PE, Rubio JCC, Reis P, Davim JP. Drilling of fiber reinforced plastics : A review. *J Mater Process Tech* 2007;186:1–7. doi:10.1016/j.jmatprotec.2006.11.146.
- [30] Bajpai PK, Debnath K, Singh I. Hole making in natural fiber-reinforced polylactic acid laminates. *J Thermoplast Compos Mater* 2017;30:30–46. doi:10.1177/0892705715575094.
- [31] Díaz-Álvarez A, Rubio-López Á, Santiuste C, Miguélez MH. Experimental analysis of drilling induced damage in biocomposites. *Text Res J* 2017:4051751772511.

doi:10.1177/0040517517725118.

- [32] Heisel U, Pfeifroth T. Influence of point angle on drill hole quality and machining forces when drilling CFRP. *Procedia CIRP* 2012;1:471–6. doi:10.1016/j.procir.2012.04.084.
- [33] Shetty N, Shahabaz SM, Sharma SS, Divakara Shetty S. A review on finite element method for machining of composite materials. *Compos Struct* 2017;176:790–802. doi:10.1016/j.compstruct.2017.06.012.
- [34] Ng S, Lau KJ, Tse PC. 3D finite element analysis of tensile notched strength of 2 / 2 twill weave fabric composites with drilled circular hole. *Compos Part B* 2000;31:113–32.
- [35] Mahdi M, Zhang L. A finite element model for the orthogonal cutting of fiber-reinforced composite materials. *J Mater Process Technol* 2001;113:373–7. doi:10.1016/S0924-0136(01)00675-6.
- [36] Arola D, Ramulu M. Orthogonal cutting of fiber-reinforced composites: A finite element analysis. *Int J Mech Sci* 1997;39:597–613. doi:10.1016/S0020-7403(96)00061-6.
- [37] Santiuste C, Soldani X, Miguélez MH. Machining FEM model of long fiber composites for aeronautical components. *Compos Struct* 2010;92:691–8. doi:10.1016/j.compstruct.2009.09.021.
- [38] Soldani X, Santiuste C, Muñoz-Sánchez A, Miguélez MH. Influence of tool geometry and numerical parameters when modeling orthogonal cutting of LFRP composites. *Compos Part A Appl Sci Manuf* 2011;42:1205–16. doi:10.1016/j.compositesa.2011.04.023.
- [39] Feito N, Díaz-álvarez J, López-puente J, Miguelez MH. Experimental and numerical analysis of step drill bit performance when drilling woven CFRPs. *Compos Struct* 2018;184:1147–55. doi:10.1016/j.compstruct.2017.10.061.
- [40] Durão LMP, de Moura MFSF, Marques AT. Numerical simulation of the drilling process on carbon/epoxy composite laminates. *Compos Part A Appl Sci Manuf* 2006;37:1325–33. doi:10.1016/j.compositesa.2005.08.013.
- [41] Singh I, Bhatnagar N, Viswanath P. Drilling of uni-directional glass fiber reinforced plastics: Experimental and finite element study. *Mater Des* 2008;29:546–53. doi:10.1016/j.matdes.2007.01.029.
- [42] Isbilir O, Ghassemieh E. Numerical investigation of the effects of drill geometry on drilling induced delamination of carbon fiber reinforced composites. *Compos Struct* 2013;105:126–33. doi:10.1016/j.compstruct.2013.04.026.
- [43] Phadnis VA, Makhdam F, Roy A, Silberschmidt V V. Drilling in carbon/epoxy composites: Experimental investigations and finite element implementation. *Compos Part A Appl Sci Manuf* 2013;47:41–51. doi:10.1016/j.compositesa.2012.11.020.
- [44] Feito N, López-Puente J, Santiuste C, Miguélez MH. Numerical prediction of delamination in CFRP drilling. *Compos Struct* 2014;108:677–83. doi:10.1016/j.compstruct.2013.10.014.
- [45] Barros JAO, Silva FDA, Toledo Filho RD. Experimental and numerical research on the potentialities of layered reinforcement configuration of continuous sisal fibers for thin mortar panels. *Constr Build Mater* 2016;102:792–801. doi:10.1016/j.conbuildmat.2015.11.018.
- [46] Rubio-López A, Hoang T, Santiuste C. Constitutive model to predict the viscoplastic behaviour of natural fibres based composites. *Compos Struct* 2016;155:8–18.

doi:10.1016/j.compstruct.2016.08.001.

- [47] Dassault. ABAQUS User's Manual. ABAQUS/CAE User's Man 2012:1–847.
- [48] Amiri A, Triplett Z, Moreira A, Brezinka N, Alcock M, Ulven CA. Standard density measurement method development for flax fiber. *Ind Crops Prod* 2017;96:196–202. doi:10.1016/j.indcrop.2016.11.060.
- [49] Faruk O, Bledzki AK, Fink H, Sain M. Progress in Polymer Science Biocomposites reinforced with natural fibers : 2000 – 2010. *Prog Polym Sci* 2012;37:1552–96. doi:10.1016/j.progpolymsci.2012.04.003.
- [50] Yan L, Chouw N, Jayaraman K. Composites : Part B Flax fibre and its composites – A review. *Compos Part B* 2014;56:296–317. doi:10.1016/j.compositesb.2013.08.014.
- [51] Fiore V, Calabrese L, Scalici T, Bruzzaniti P, Valenza A. Experimental design of the bearing performances of flax fiber reinforced epoxy composites by a failure map. *Compos Part B* 2018;148:40–8. doi:10.1016/j.compositesb.2018.04.044.
- [52] Rubio-López A, Olmedo A, Díaz-Álvarez A, Santiuste C. Manufacture of compression moulded PLA based biocomposites: A parametric study. *Compos Struct* 2015;131:995–1000. doi:10.1016/j.compstruct.2015.06.066.
- [53] Liu DF, Tang YJ, Cong WL. A review of mechanical drilling for composite laminates. *Compos Struct* 2012;94:1265–79. doi:10.1016/j.compstruct.2011.11.024.
- [54] Kumar D, Sing KK. Experimental analysis of Delamination, Thrust Force and Surface roughness on Drilling of Glass Fibre Reinforced Polymer Composites Material Using Different Drills. *Mater Today Proc* 2017;4:7618–27. doi:10.1016/j.matpr.2017.07.095.
- [55] Gaugel S, Sripathy P, Haeger A, Meinhard D, Bernthaler T, Lissek F, et al. A comparative study on tool wear and laminate damage in drilling of carbon-fiber reinforced polymers (CFRP). *Compos Struct* 2016;155:173–83. doi:10.1016/j.compstruct.2016.08.004.